Supplementary Material

Section I: Methods

Northern blot analysis. Total RNA was isolated from *B. subtilis* 168 cells grown in LB-medium at 37°C using the single step method (Chomzynski and Sacchi, 1987). 3 µg of total RNA was separated on 8% denaturing (8 M urea) polyacrylamide (PAA) gels. Gels were washed for 5 min in 0.5 x TBE and RNA was transferred overnight to a positively charged nylon membrane (Roche) by semidry blotting in 0.5 x TBE at 3.75 mA/cm^2. Northern hybridization was performed using the Northern Starter Kit (Roche) following the manufacturer's instructions. Fully complementary, DIG-labeled RNA was used as probe for 6S-1 RNA. Detection of pRNA transcripts was performed as described previously (Beckmann *et al*., 2010). For outgrowth experiments, cells in late stationary phase were diluted 1:5 in fresh prewarmed (37°C) LB-medium and samples were taken from 2 min to 4 h after dilution. Rifampicin was added with the dilution medium to a final concentration of 100 µg/ml.

Structure probing. 6S-1 RNA was transcribed *in vitro* using T7 run-off transcription. The DNA template for transcription was generated by PCR from genomic *B. subtilis* 168 DNA (6S-1: primers 5'-TAA TAC GAC TCA CTA TAG GAG TCC TGA TGT GTT AGT TGT ACA CCT AG-3' and 5'-AAA GTC CCA ATA GTG CCG TTG-3'; T7 promoter sequence underlined). Transcription reactions contained 8 mM guanosine as initiator nucleoside to generate transcripts with 5'-OH ends for direct 5'-endlabeling. For 5'-endlabeling, 60 pmol 6S-1 RNA, 10 U T4 polynucleotidkinase (PNK, Fermentas) and 3 µl of (γ-^{32}P)-ATP (3000 Ci/mmol) were incubated in a volume of 15 µl 1 x PNK buffer (Fermentas) for 90 min at 37°C. RNA was purified by denaturing (8 M urea) PAGE, gel-extracted overnight in 1 M NaOAc pH 4.9 at 8°C, and concentrated by ethanol precipitation before probing. For all probing experiments, 10 pmol of unlabeled RNA together with trace amounts (20,000 Cerenkov cpm) of labeled RNA were used. Probed RNA was separated on thin (0.5 mm) 12% polyacrylamide gels containing 8 M urea and hydrolysis patterns were analyzed with a Bio-Imaging Analyzer FLA-3000-2R (Fujifilm). RNase T1 and V1 digestions were performed under native conditions [50 mM HEPES pH 7.9, 4.5 mM $Mg(OAc)_2$, 100 mM NH_4OAc]. RNase T1 digestion was further conducted under denaturing conditions (20 mM Na-Citrate pH 5.0, 7 M urea, 1 mM

EDTA). After preincubation of the RNA in the respective buffer for 10 min at 37°C, 0.8 U RNase T1 (0.05 U RNase V1) were added and samples were incubated in a final volume of 50 µl at 37°C for 20 min (7 min for RNase V1). Reactions were stopped by addition of 15 µl 0.45 M NH_4OAc and ethanol precipitation. Lead cleavage was performed in PA buffer (50 mM Tris-HCl pH 7.5, 100 mM NH_4Cl). After preincubation of the RNA in PA buffer for 10 min at 37°C, 250 µM $Pb(OAc)_2$ was added and samples were incubated in a final volume of 100 µl for 3 min at 37°C. Reactions were stopped by addition of 20 µl 2 mM EDTA, followed by ethanol precipitation. Alkaline hydrolysis of RNA was performed in alkaline buffer (50 mM $NaHCO_3$) in a volume of 13 µl for 8 min at 100°C. Reactions were stopped by adding 13 µl 10 mM EDTA, followed by ethanol precipitation. For 3'-endlabeling, we employed a 6S-1 RNA carrying an HDV ribozyme at its 3'-end in order to generate homogeneous 3'-ends derived from HDV *cis*-cleavage. For this purpose, the *bsrA* gene was amplified by PCR (primers 5'-AAA GTC CCA ATA GTG CCG TTG-3' and 5'-CAG GAA TTC TAA TAC GAC TCA CTA TAG GAG TCC TGA TGT GTT AGT TGT ACA CCT AG-3'). Next, the HDV coding sequence was amplified (primers 5'-CAA CGG CAC TAT TGG GAC TTT GGC CGG CAT GGT CCC AG-3' and 5'-GGC CAG TGC CAA GCTT GTC CCA TTC GCC ATT ACC GAG-3') and both PCR products were combined for overlap extension PCR resulting in the final T7-*bsrA*-HDV product which was cloned into the pUC18 vector using *Eco*RI and *Hind*III restriction sites. After T7 transcription, the released 6S-1 RNA was eluted from the gel and its 2',3'-cyclic phosphate ends were removed using 20 U T4 PNK in 100 mM imidazole pH 6.0, 100 µM ATP, 10 mM $MgCl_2$ 0.07% (v/v) 2-mercaptoethanol and 20 ng/µl BSA (final volume 100 µl, 6 h at 37°C). 3'-Endlabeling was performed using 10 U T4 RNA ligase (Fermentas) and 3 µl of (5'-^{32}P)pCp (3000 Ci/mmol) in a final volume of 15 µl in 1 x ligation buffer (Fermentas) overnight at 10°C before probing was performed as described above.

Construction of the U136/U145U/A146 mutant 6S-1 RNA. The gene for the mutant 6S-1 RNA was constructed by site-directed mutagenesis. For this purpose, 5'-phosphorylated primers #56_6S-1U136_U145_A146_fw (5'- CCA C<u>T</u>T GCT GAG A<u>TA</u> GGG TTC AAA AC -3; mutations underlined) and #57_6S-1U136_U145_A146_rv (5'-GTG CCC TCT TTT AAA TCT TGT AAG TCC TC -3') were annealed to opposite strands of plasmid pBB1 (pUC18 derivative, contains the *bsrA* gene encoding mature 6S-1 RNA under control of the phi10 T7 promoter; Amp^R) within the *bsrA* gene, with the

primer 5'-ends positioned in a head-to-head fashion. After a PCR reaction, 30 x [98°C for 30 s (20 s after cycle 1), 55°C for 30 s, 72°C for 100 s] and finally 8 min at 72°C, the product was purified with the PCR Purification Kit (Qiagen), followed by *Dpn*I (Fermentas) digestion of the parental DNA strands and again purification with the aforementioned kit. Finally, the blunt ends of the amplified plasmid were ligated with T4 DNA ligase (Fermentas), followed by transformation of *E. coli* DH5α cells according to standard procedures. Recombinant plasmids encoding the mutant 6S-1 RNA, isolated from individual cell clones, were verified by DNA custom sequencing (Eurofins MWG Operon), and the mutant 6S-1 RNA was transcribed with T7 RNA polymerase from plasmid pBB1_bsrA_U136/U145U/A146 after linearization with *Hind*III (Fermentas).

Bioinformatics. To derive a model for the pRNA-induced structural rearrangement in 6S-1 RNA, we compared our structural probing data with different constraints of the *RNAsubopt -C* (Lorenz et al., 2011) output. To explore whether the conformational rearrangement observed for *B. subtilis* 6S-1 RNA may be phylogenetically conserved, we downloaded a secondary structural alignment of all deposited bacterial 6S RNAs from Rfam v.10.0 (Gardner *et al.*, 2009) (output file **RF00013_seed.stk**). By manually adding *Aquificales* sequences, the alignment increased to 162 sequences. We performed three steps: (1) *Negative control:* To simulate the ground state (no pRNA present and no structural rearrangement), we analyzed the potential of the 3'-part of the central bulge (corresponding to nt 134-147 of *B. subtili*s 6S-1 RNA; Fig. S3 B) to form a helix using the program RNAfold v.2.0 (Lorenz et al., 2011). For 54 out of 162 6S RNA sequences, a hairpin-like structure (at least two interacting base pairs with negative minimum free energy) was evident (with mostly marginal low energy values: μ = -0.54 kcal/mol, standard deviation = 0.91 kcal/mol). (2) *Positive control:* For a simulation of pRNA:6S RNA hybrids we extended our region of unpaired nucleotides (mimicking pRNA-induced disruption of the closing stem), testing for potential hairpin formation in the region corresponding to nt 134-157 of *B. subtilis* 6S-1 RNA. Surprisingly, 161 out of 162 sequences had the potential to form a persistent hairpin with μ = -7.80 kcal/mol (standard deviation = 4.10 kcal/mol), with the colour code in Fig. S3 A indicating the individual hairpin stability. Only *Oceanobacillus iheye* did not show at least four interacting base pairs. (3) *Collapse of central bulge:* in this third setup, we analyzed if the upper part of the central bulge (nt 41 to 53 in *B. subtilis* 6S-1 RNA) has the potential to base-pair with nucleotides in the 3'-portion of the closing stem (nt 148 to 171 in *B.*

subtilis 6S-1 RNA) that become accessible after stem disruption as a result of pRNA invasion. For 147 of the 162 sequences such a bulge collapse with < -1.30 kcal/mol was found to be possible, the majority of them being plausible (μ = -5.70 kcal/mol; standard deviation = 3.48 kcal/mol; Fig. S3 A, squares). This also included *Aquifex aeolicus* (Willkomm et al., 2005), for which we identified the pRNA sequence by deep sequencing (data not shown). All input and output files can be obtained at the Supplement web page.

RNA decay experiments. 10 OD_{600} of *B. subtilis* cells were harvested 3 min after induction of outgrowth in LB medium (see above, “Northern blot analysis”). The cell pellet was snap frozen in liquid nitrogen and stored at -80°C. Then, the pellet was resuspended in 200 µl of CE-lysis buffer (20 mM Tris-HCl pH 8.0, 150 mM KCl, 1 mM $MgCl_2$, 1 mM DTT, 0.5 mg/ml lysozyme). The mixture was transferred to a 2 ml screw-capped tube and an equivalent of 200 µl glass beads (diameter 0.1 mm) was added. Cell lysis was performed in a FastPrep®-24 instrument (MP Biomedicals) device with six times 30 s bursts (speed: 6.0 m/s) with 15 s on ice in between. Another 200 µl of CE-lysis buffer was added and the lysate was centrifuged for 10 min at 13.000 rpm and 4°C in a table-top centrifgue. Around 450 µl of cleared lysate was transfered to a 1.5-ml tube and 5' endlabeled 6S-1 RNA was added, either in its free form or annealed to pRNA (see Materials and Methods section of the main text, “6S1 RNA:pRNA annealing”). Aliquots were taken at different time points (from 2 to 30 min) and immediately mixed with 1 volume of phenol to stop 6S-1 RNA decay; phenol was added prior to the 6S-1 RNA in the case of the control (Fig. S4, “ctr“). Extracted total RNAs, concentrated by ethanol precipitation, were then analyzed on 1 mm thick 10% denaturing polyacrylamide gels and visualized with a Bio-Imaging Analyzer (Fig. S4 B) as described under “Structure Probing“ above.

Section II: Supplementary Figures

Supplementary figure legends

Fig. S1. Structure and function of a circularly permuted 6S-1 RNA. (**A**) Construction strategy: two copies of *bsrA* encoding 6S-1 RNA were inserted into pUC18 via *Eco*RI/*Hind*III and *Hind*III to generate plasmid pBB6. Using pBB6 as template, a PCR product for T7 transcription was generated using primers bsrAcpT7 fw (5'-TAA TAC GAC TCA CTA TAG GTA AAG AGG ACT TAC AAG ATT TAA AA) and bsrAcprev (5'-GAA TGA AAA GAG GCA TGT ACG). (**B**) Secondary structure of wild-type 6S-1 RNA (6S-1 wt) and the circularly permuted mutant variant (6S-1 cp). Numbering of 6S-1 cp is indicated as for the wild-type 6S-1 RNA. The *Hind*III site served as a linker to connect the original 5'- and 3'-ends of the wild-type RNA. Black arrows mark the start for pRNA synthesis. (**C**) Capability of 6S-1 cp RNA to bind to the σ^A-RNAP and to form the rearranged structure upon binding of the pRNA 14-mer. Trace amounts (< 1 nM) of 5'-endlabeled 6S-1 cp RNA and 1.7 µM unlabeled 6S-1 cp RNA, either alone (lane 3) or in the presence of 17 µM pRNA 14-mer (lane 4), were annealed in 6 µl 1 x TE buffer and then loaded on the 7.5% native PAA gel; lanes 1 and 2: as lanes 3 and 4, but before gel loading 1 µl of a heparin solution (400 ng/µl) and 2 µl 5 x activity buffer were added and samples were kept at 37°C; then 1.06 µl RNAP holoenzyme (8 µg/µl) was added and samples were incubated for 30 min at 37°C followed by gel loading.

Fig. S2. The all-LNA 8-mer (5'-GTTCGGTC) is able to induce the structural rearrangement in 6S-1 RNA (3'-endlabeled). Samples loaded in lanes 1 to 5 were prepared as lanes 1 to 5 in Fig. 3 C of the main manuscript. A comparable probing experiments with the corresponding RNA 8-mer failed to affect 6S-1 RNA structure (data not shown).

Fig. S3. (**A**) *In silico* prediction of pRNA-induced rearrangements in the structural core of bacterial 6S RNAs. The figure shows a phylogenetic tree of 6S RNA sequences (obtained from Rfam, *RF00013 seed.stk*; Gardner *et al*., 2009), using the program SplitsTree (Hudson and Bryant, 2006). Stabilities of the predicted hairpin structures are differentiated by the colour code ranging from -0.40 kcal/mol (dark blue) to -9.50

kcal/mol (red). The potential to undergo the central bulge collapse is indicated by squares in the case of energy values below -1.30 kcal/mol (circled otherwise). Hairpin stabilities are relatively uniform within bacterial branches; γ-proteobacteria have the potential to form the most stable hairpins. Input and output files can be obtained at the Supplement web page (http://bioinf.pharmazie.uni-marburg.de/supplements/136). (**B**) Predicted structural rearrangements of 6S RNAs with known pRNA sequences (*B. subtilis* 6S-1 RNA, *E. coli* and *Aquifex aeolicus* 6S RNA). *B. subtilis* 6S-1 RNA represents a group of 6S RNAs for which the hairpin is predicted to be formed (at least partially) already in the free RNA; here, the central bulge collapse appears to be the major component of the rearrangement. In other bacteria, such as *E. coli* representing the γ-proteobacteria, stable formation of an extended hairpin is predicted to occur only after pRNA-induced disruption of 6S RNA structure; here, the extended hairpin is particularly stable and a central bulge collapse is not predicted to occur. In a third group of 6S RNAs, such as the one from *Aquifex aeolicus*, both mechanistic components, pRNA-induced hairpin formation and central bulge collapse seem to be implemented simultaneously. For further details, see main manuscript.

Fig. S4. Rifampicin treatment and pRNA annealing had no effect on 6S-1 RNA decay rates. (**A**) The central panel shows an 8% native PAGE analysis of 5'-endlabeled 6S-1 RNA (160 nM) annealed to the pRNA in the presence of either 0, 80, 160, 400, 800 or 1600 nM pRNA 14-mer (for details, see “6S-1 RNA:pRNA annealing” in the Materials and Methods section of the main manuscript). (**B**) 5’-endlabeled 6S-1 RNA (65 nM) was subjected to the annealing procedure either in absence of the pRNA 14-mer (left gel image) or in the presence of a 10-fold molar excess of the 14-mer (central gel image) in a total volume of 15 µl, followed by addition of 450 µl of cleared lysate from outgrowth bacteria treated with rifampicin or not. Incubation at 37°C was stopped after 2, 5, 10, 20 or 30 min as indicated above lanes; ctr = reaction stopped by addition of phenol before addition of labeled 6S-1 RNA. The total radioactivity of each lane and that of the corresponding intact 6S-1 RNA band were quantified using a Bio-Imaging Analyzer FLA-3000-2R (Fujifilm) and the analysis software PCBAS/AIDA (Raytest). The fraction of intact 6S-1 RNA (the radioactivity representing intact 6S-1 RNA divided by the radioactivity of the entire lane) was calculated. Fraction values were further normalized to the value for the ctr lane which was set to 1. The normalized fractions (relative degradation) were plotted as a function of time (plot on the right).

Fig. S5. (**A**) Base-pairing probabilities of free *H. pylori* (strain 26695) 6S RNA, and of the same 6S RNA where either the sequence encoding the pRNA 12-mer or the pRNA* 17-mer is blocked (via constraint folding) for intramolecular base-pairing; shown are the RNAfold predictions for the minimal free energy (MFE) structure and centroid (CT) secondary structure as the best representative of a set of structures ("Boltzmann ensemble") with similar ΔG values. For paired nucleotides, orange to red indicates high and blue to purple low base-pairing probabilities; for unpaired regions, the colour denotes the probability of being unpaired. The coding sequences for the pRNA 12-mer and pRNA* 17-mers are marked by thick black lines along the structure. The extended hairpin is contoured by thin black lines. (**B**) Folding dot plots (RNAfold) corresponding to the structures shown in panel A. (**C**) Folding dot plots predicted by mfold; here the nucleotides encoding the pRNA 12-mer or the pRNA* 17-mer were replaced by N's to mimic blockage of these regions by pRNA association.

References

Beckmann BM, Grünweller A, Weber MHW, Hartmann RK (2010) Northern blot detection of endogenous small RNAs (14 nt) in bacterial total RNA extracts. *Nucleic Acids Res* **38**:e147.

Chomzynski P, Sacchi N (1987) Singlestep method of RNA isolation by acid guanidinium thiocyanatephenolchloroform extraction. *Anal Biochem* **162**:156-159.

Gardner PP, Daub J, Tate JG, Nawrocki EP, Kolbe DL, Lindgreen S, Wilkinson AC, Finn RD, GriffithsJones S, Eddy SR, Bateman A (2009) Rfam:updates to the RNA families database. *Nucleic Acids Res* **37**:D136-140.

Hudson DH, Bryant D (2006) Application of Phylogenetic Networks in Evolutionary Studies. *Mol Biol Evol* **23**:254-267.

Lorenz R, Bernhart SH, Hoener Zu Siederdissen C, Tafer H, Flamm C, Stadler PF, Hofacker IL (2011) ViennaRNA Package 2.0. Algorithms Mol Biol. 6(1):26. [Epub ahead of print].

Willkomm DK, Minnerup J, Hüttenhofer A, Hartmann RK (2005) Experimental RNomics in Aquifex aeolicus: identification of small noncoding RNAs and the putative 6S RNA homolog. *Nucleic Acids Res* **33**:1949-1960.

A

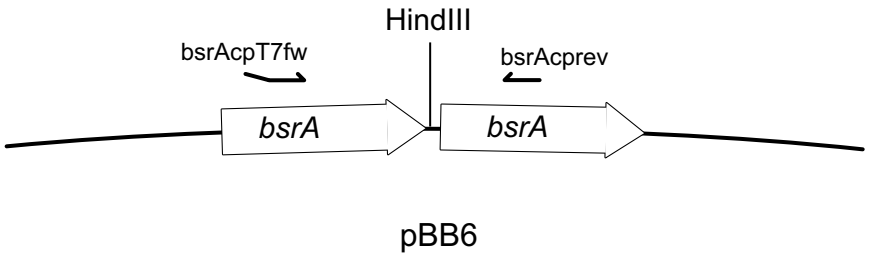

pBB6

B

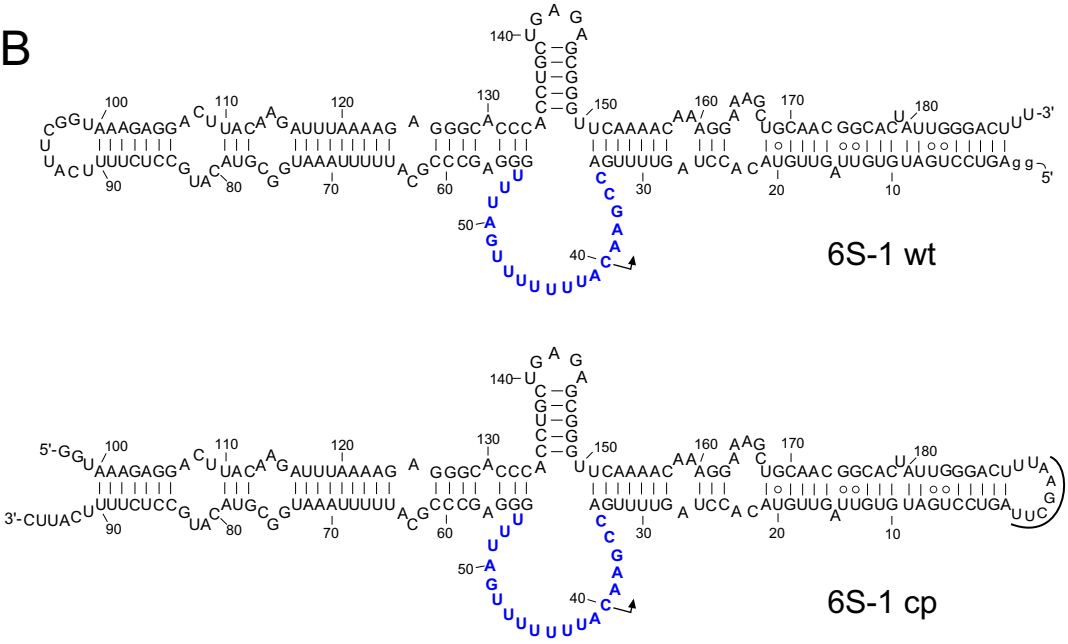

C

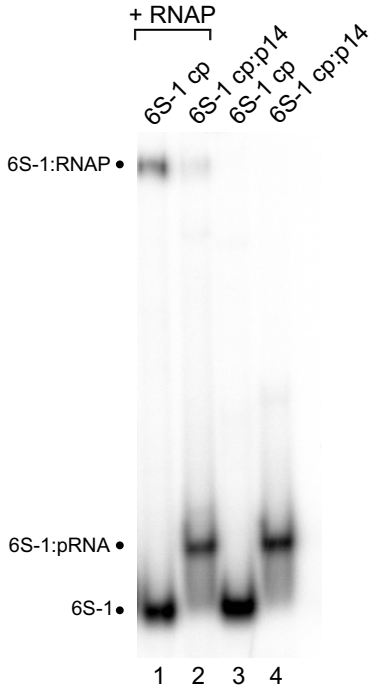

Fig. S1

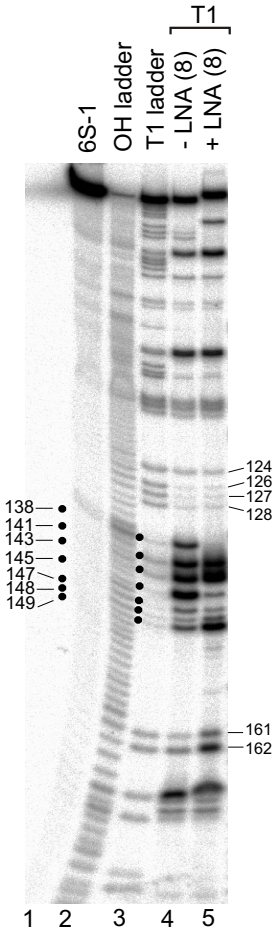
6S-1
OH ladder
T1 ladder
T1
- LNA (8)
+ LNA (8)
138
141
143
145
147
148
149
124
126
127
128
161
162
1 2 3 4 5

Fig. S2

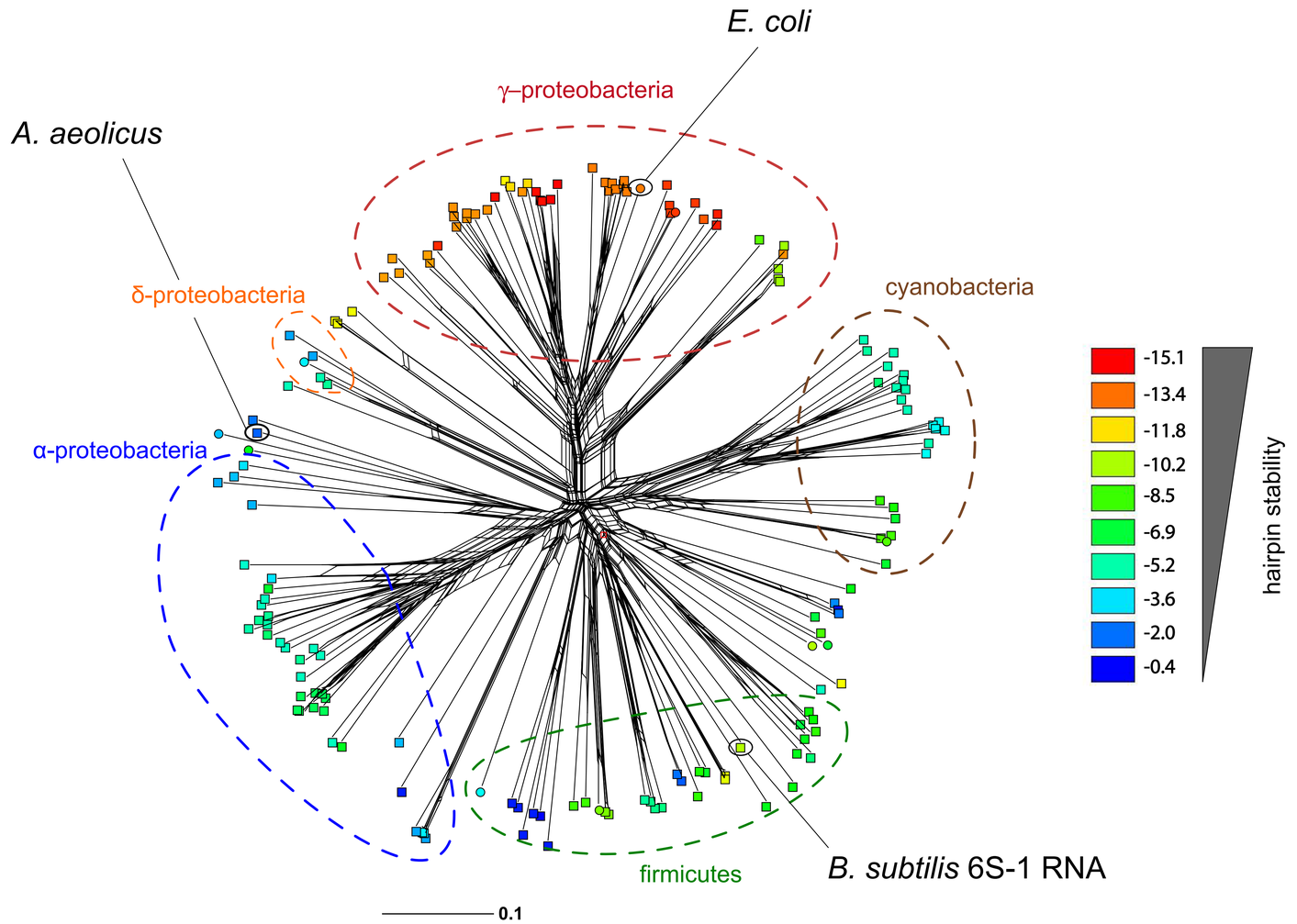
E. coli
γ–proteobacteria
A. aeolicus
δ-proteobacteria
cyanobacteria
α-proteobacteria
firmicutes
B. subtilis 6S-1 RNA
0.1
-15.1
-13.4
-11.8
-10.2
-8.5
-6.9
-5.2
-3.6
-2.0
-0.4
hairpin stability

Fig. S3 A

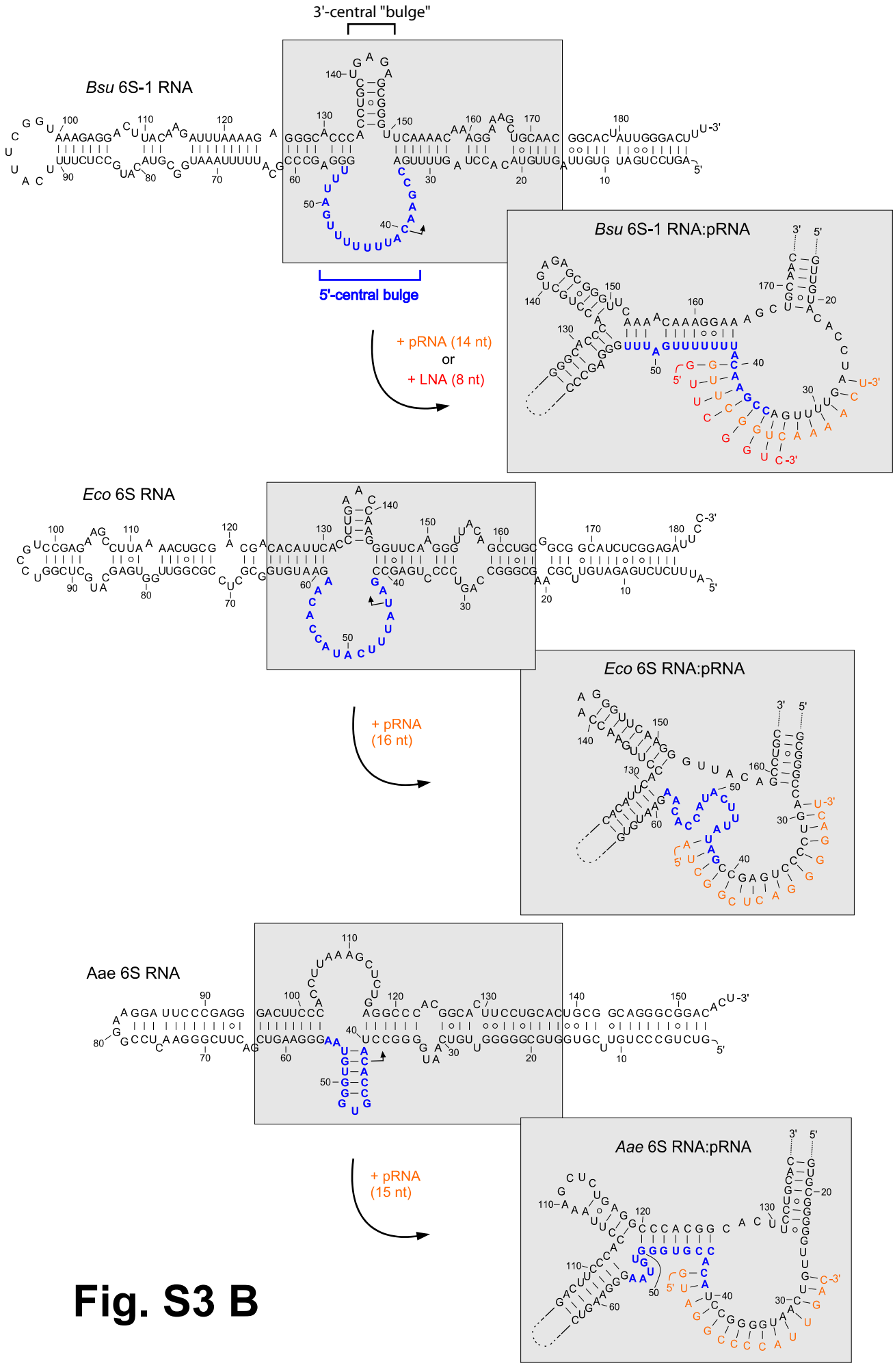
3'-central "bulge"
Bsu 6S-1 RNA
5'-central bulge
+ pRNA (14 nt)
or
+ LNA (8 nt)
Bsu 6S-1 RNA:pRNA
Eco 6S RNA
+ pRNA
(16 nt)
Eco 6S RNA:pRNA
Aae 6S RNA
+ pRNA
(15 nt)
Aae 6S RNA:pRNA

Fig. S3 B

A

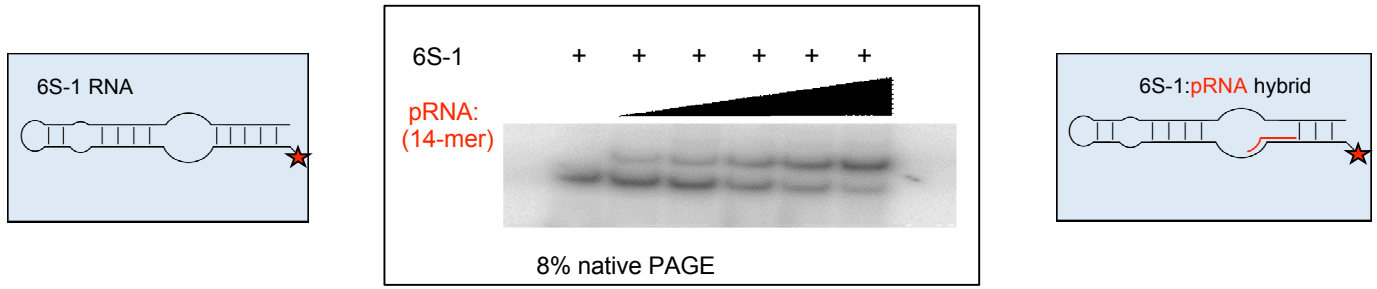
6S-1 RNA
6S-1
+ + + + + +
pRNA:
(14-mer)
8% native PAGE
6S-1:pRNA hybrid

B

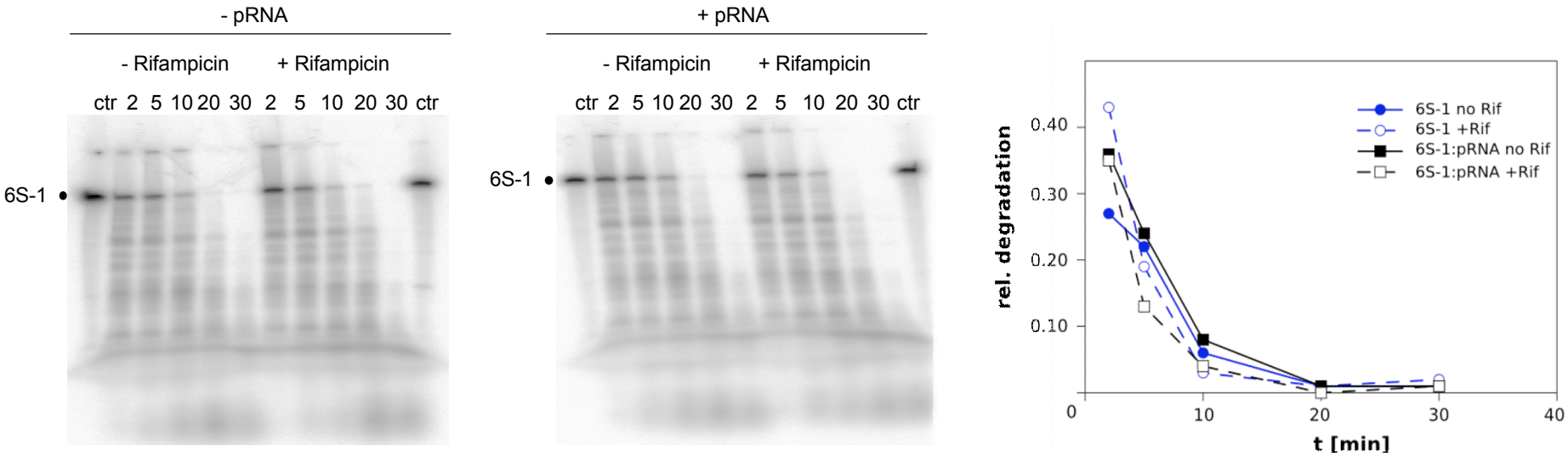
- pRNA
+ pRNA
- Rifampicin
+ Rifampicin
ctr 2 5 10 20 30 2 5 10 20 30 ctr
6S-1
rel. degradation
t [min]
6S-1 no Rif
6S-1 +Rif
6S-1:pRNA no Rif
6S-1:pRNA +Rif

Fig. S4

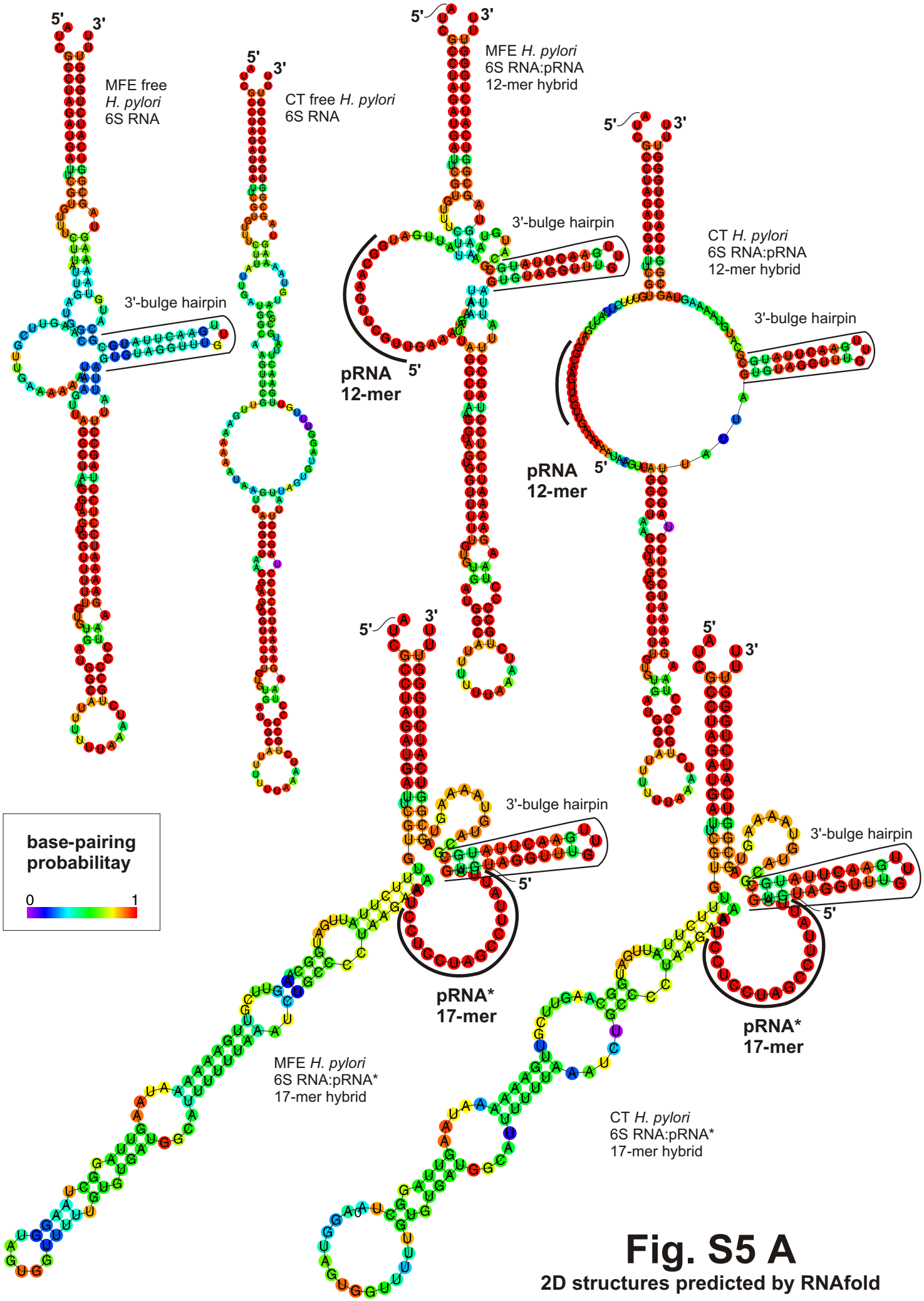

Fig. S5 A

2D structures predicted by RNAfold

H. pylori (strain 26695) free 6S RNA

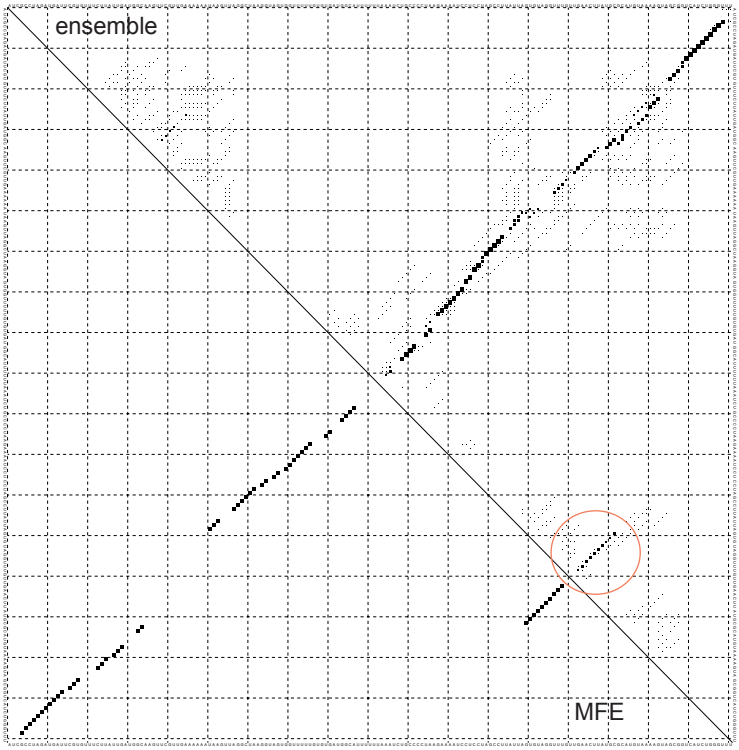

H. pylori 6S RNA, the 12 pRNA-coding nucleotides blocked for intramolecular base-pairing

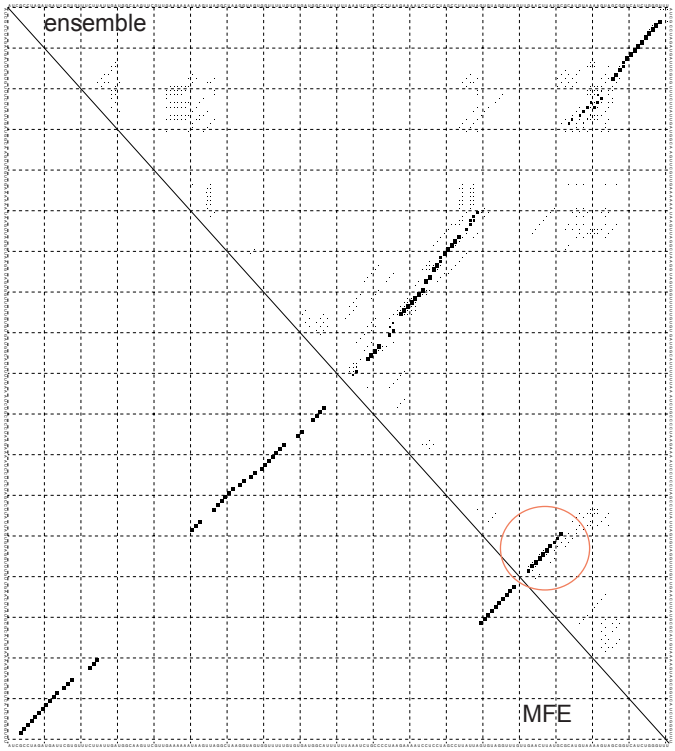

H. pylori 6S RNA, the 17 pRNA*-coding nucleotides blocked for intramolecular base-pairing

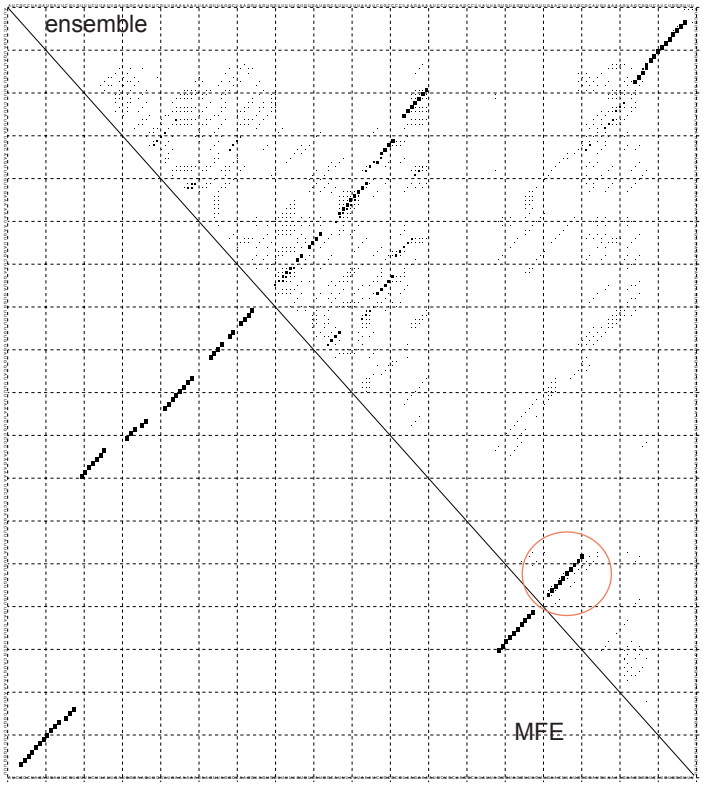

Fig. S5 B

Folding dot plots predicted by RNAfold

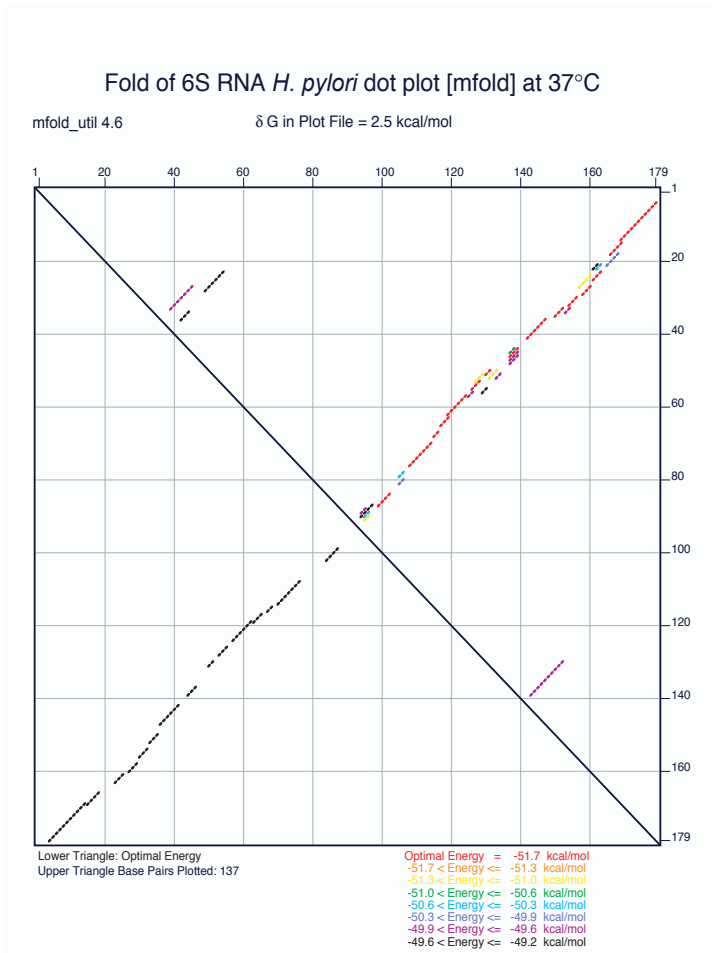

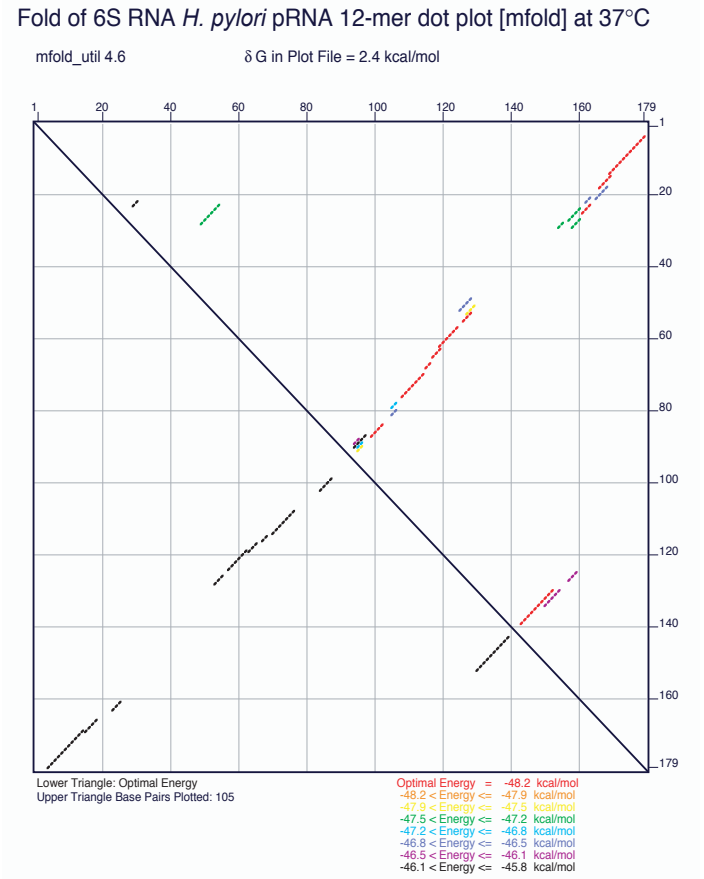

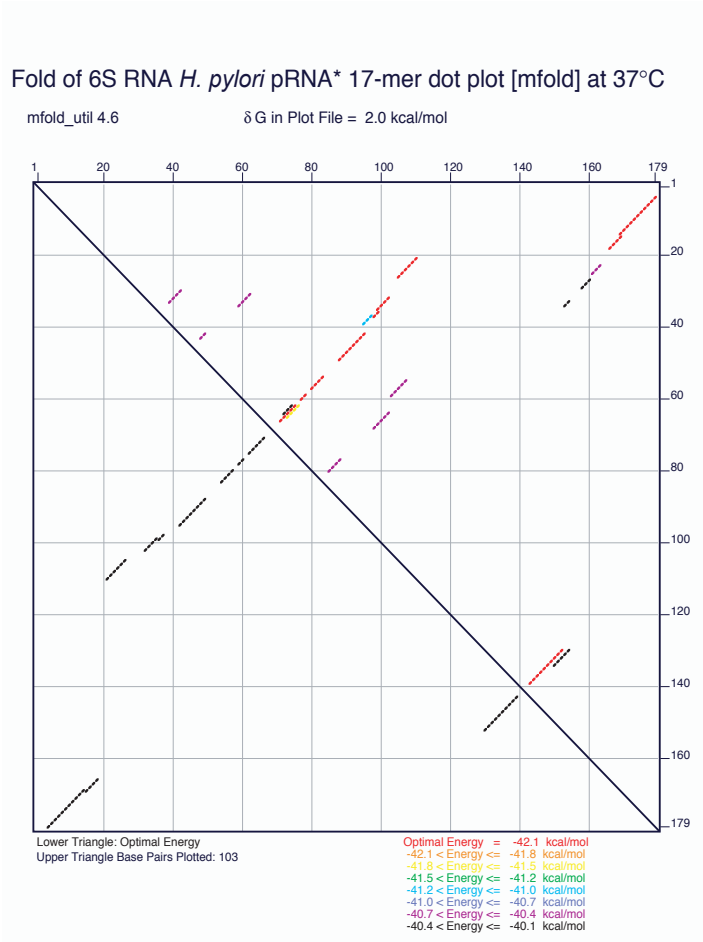

Fig. S5 C

Folding dot plots predicted by mfold